A COOPERATIVE CONTROL FOR CAR SUSPENSION AND BRAKE SYSTEMS

C. NOUILLANT[1,2]*, F. ASSADIAN[1], X. MOREAU[2] and A. OUSTALOUP[2]

[1]PSA Peugeot Citroën, Route de Gizy, 78943 Vélizy - Villacoublay, France
[2]Laboratoire d'Automatique et de Productique Université Bordeaux I-ENSEIRB
351 cours de la Libération, 33405 Talence cedex, France

ABSTRACT–Mechatronic subsystems are more and more developed in automotive industries. To enhance the local controls performances, a cooperative control between ABS and Suspension systems is proposed. The respective controls are first designed separately with their dedicated models. Then a hybrid hierarchical architecture is developed. The advantage of this architecture is discussed through vehicle performance with simulation results.

KEY WORDS : Anti-lock braking system, Active vehicle suspension, Robust control, Feedforward control, Finite state machine, Vehicle dynamics

NOMENCLATURE

Front	: $i=1$; Rear: $i=2$
f_{Li}, f_{Ni}	: longitudinal and normal tire forces
Γ_{bi}	: braking torque
a_x, v_x	: vehicle longitudinal acceleration and speed
ω_{1i}	: wheel angular velocities
z_{0i}, v_{0i}	: vertical road displacement and speed
z_{1i}	: vertical displacement of unsprung masses
z_{3i}, z_G	: vertical displacements on sprung mass
θ_G	: pitch angle
u_i	: control forces from suspension
f_{0i}	: sprung mass vertical disturbance forces
λ_i	: tire slip-ratio
μ_i	: tire-road coefficient of friction
M	: vehicle total mass
m_2, m_{1i}	: sprung mass and unsprung masses
I_y	: vehicle pitch rotational inertia
I_i	: wheel rotational inertia
R_i	: wheel radii
a, b	: center of gravity - front/rear axles longitudinal distances
h	: height of the center of gravity
k_{1i}, k_{2i}	: tire and suspension stiffnesses
b_{2i}	: suspension damping
S_{vi}	: suspension piston section
q_{suspi}	: suspension flows
α_i	: criteria weights

J_i	: criteria for suspension feedback control
m^{opt}_i	: optimal fractional derivative order for CRONE suspension controller
D_{pedal}	: brake pedal displacement
B	: brake fluid constant
c_1	: master cylinder viscous coefficient
c_{2i}	: secondary cylinder viscous coefficient
F_{diski}	: force on the brake disk
F_{mc}	: force generated by the master cylinder
H_{brake0}	: servo-valve with current amplifier equivalent gain
I_{hi}	: fluid line inertia
k_{2i}, k_{2i}^0	: non-linear and linearized springs
K_{assist}	: pedal displacement to master cylinder force equivalent gain
K_{ei}	: hydraulic brake circuit steady state gain
m_{p1}	: master cylinder piston mass
m_{p2i}	: secondary cylinder piston mass
P_1	: master cylinder fluid pressure
P_{1i}	: distributed pressure from master cylinder
P_{2i}	: secondary cylinder pressure
P_{ABSi}	: pressure drop caused by ABS
Q_i	: hydraulic line flow
R_e	: equivalent radius of the brake disk
r_{hi}	: fluid line resistance
R_i	: radius of the wheel
S_1	: master cylinder section
S_{2i}	: secondary cylinder section
V_1	: master cylinder fluid volume
V_{2i}	: secondary cylinder fluid volume

Corresponding author. e-mail: cedric.nouillant@mpsa.com

x_1 : master cylinder piston displacement

x_{2i} : secondary cylinder piston displacement

x_i^0 : residual piston displacement

μ_e : caliper-disk coefficient of friction

ω_r : wheel rotational speed reference

γ_j : interpolation polynomial coefficients

n_{ABS}, n_{susp} : fractional derivative order for ABS and suspension open-loops

1. INTRODUCTION

In the last decades, mechatronic subsystems have been extensively developed in automotive applications as they increase system performance compared to passive components (Dreyer *et al.*, 1992). However, they often fulfil a single dedicated function, such as controllable dampers of vehicle suspension. According to the future prospects (Hamrs, 2001), a cooperative control between ABS and suspensions systems will enhance vehicle global performances.

First, vehicle dynamics and brake system models are introduced. The suspension is composed of a continuously controllable damper (Abadie, 1998) and a low frequency active device (Moreau *et al.*, 2001). The brake system has proportional servo-valves for advanced control (Assadian, 2001).

For the suspension system, two optimal strategies (one for road holding and one for passengers comfort) are designed with CRONE methodology (Oustaloup and Matthieu, 1999).

ABS also benefits from CRONE control by considering the road coefficient of friction as an uncertain parameter (Jacquet, 1996) leading to a robust performance for wheel slip regulation. A feedforward controller is also developed for enhancing performance. Thus, ABS switches logic is implemented with a finite state machine.

Because of the coupling effects between these two systems, the suspension strategy is of importance as a comfort oriented design can be a disadvantage when braking on a rough road, especially when the wheel vertical movement is severe. This problem can lead to ABS control degradation (Forkenbrock *et al.*, 1998).

To overcome this difficulty, a new cooperative control architecture between ABS and suspension system is proposed, aiming to enhance global vehicle performance (Abadie, 1999). To this end, a hybrid control architecture is developed (Riedinger, 1999), and its advantage is then proved in a critical case where the vehicle is braked on a wet and uneven road.

2. VEHICLE AND BRAKE SYSTEM MODELS
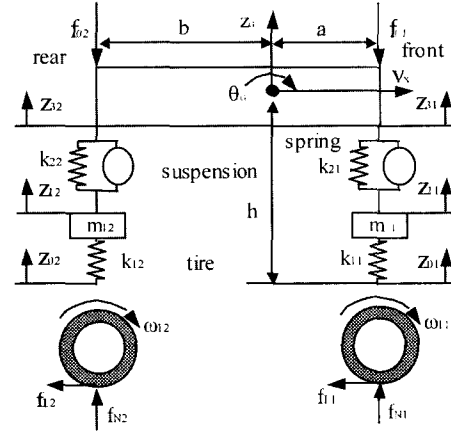
2.1. Vehicle Dynamics

Figure 1. Two-wheel car model.

The motion of the two-wheel car model, as shown in Figure 1, is described by seven differential equations (Moreau *et al.*, 2001).

2.1.1. Linear model of the vertical dynamics

The linear model of the vertical dynamics is described by four differential equations:

− unsprung masses motions

$$m_{1i}\ddot{z}_{1i}=f_{Ni}-k_{2i}(z_{1i}-z_{3i})-u_i-m_{1i}g \tag{1}$$

where f_{Ni} are the normal forces defined by

$$f_{Ni}=k_{2i}(z_{0i}-z_{1i}) \tag{2}$$

− heave motion

$$m_2\ddot{z}_G=\sum_{i=1}^{2}(k_{2i}(z_{1i}-z_{3i})+u_i-f_{0i})-m_2g \tag{3}$$

− pitch motion

$$I_y\ddot{\theta}_G=a(k_{21}(z_{11}-z_{31})+u_i-f_{01})$$
$$-b(k_{22}(z_{12}-z_{32})+u_2-f_{02}) \tag{4}$$

where $u_i(t)$ are the forces developed by dampers and load leveling devices.

The vertical front and rear forces $f_{0i}(t)$ as shown in Figure 1, include the load shift due to the longitudinal acceleration on the normal force variation, namely:

$$f_{01}(t)=-\frac{h}{a+b}Ma_x(t) \text{ and } f_{02}(t)=+\frac{h}{a+b}Ma_x(t) \tag{5}$$

2.1.2. Nonlinear model of the longitudinal dynamics

The nonlinear model of the longitudinal dynamics is described by three differential equations:

− longitudinal motion

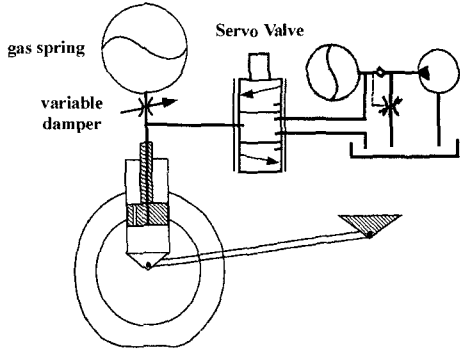$$M\dot{v}_x=f_{L1}+f_{L2} \tag{6}$$

− wheels angular motions

Figure 2. Schematic diagram of an active suspension.

$$I_i \dot{\omega}_{1i} = \Gamma_{bi} - R_i f_{Li} \tag{7}$$

The manner a tire generates forces is complicated. Pacejka's model (Pacejka and Sharp, 1991) gives a steady-state approach of the phenomena; the longitudinal force is function of the tire normal force, the tire-road coefficient of friction, and the slip-ratio. For a braked wheel, this last variable is defined as:

$$\lambda_i = 1 - \frac{R_i \omega_{1i}}{v_x} \tag{8}$$

This ratio can vary from 0% (perfect match between wheel and vehicle speeds) to 100% (the wheel is locked). The longitudinal forces can be approximated by:

$$f_{Li}(t) = \mu_i(\lambda_i) f_{Ni}(t) \tag{9}$$

2.1.3. Active suspension

A hydropneumatic suspension with the addition of load leveling active device and controllable dampers (cf. Fig. 2) forms the basis of the Williams Formula One Racing system (Wright and Williams, 1989) and is part of this study.

Whereas the controllable damper (Abadie, 1998) is a dissipative component, it can control wheel vertical displacements because of its large bandwidth. The active device is a proportional servo-valve with a limited bandwidth about 10 Hz enabling to control body movements without excessive energy consumption.
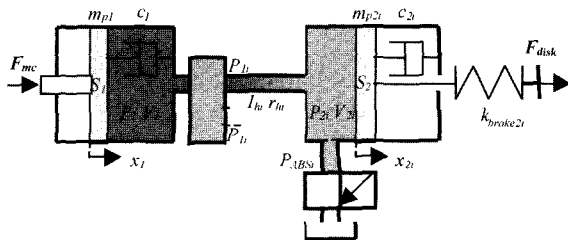

Figure 3. Hydraulic line brake model.

2.2. Braking System Model

The proposed ABS system (Assadian, 2001), in Fig. 3 is composed of high bandwidth proportional servo-valves that enable modulation of brake pressures such as EHB technology (Hamrs, 2001).

The relation between the brake pedal displacement and the force acting on the master cylinder can be modeled by a simple constant gain:

$$F_{mc} = K_{assist} \cdot D_{pedal} \tag{10}$$

The master cylinder piston movement is:

$$m_{p1} \cdot \ddot{x}_1 = F_{mc} - P_1 \cdot S_1 - c_1 \cdot \dot{x}_1 \tag{11}$$

This leads to the pressure change in the master cylinder chamber:

$$\dot{P}_1 = \frac{B}{V_1} \left(\dot{x}_1 \cdot S_1 - \sum_i Q_i \right) \tag{12}$$

Then, for the sake of simplicity, the pressure is assumed to be distributed to the front and rear hydraulic lines according to:

$$P_{11} = \frac{2}{3} \cdot P_1 \quad \text{and} \quad P_{12} = \frac{1}{3} \cdot P_1 \tag{13}$$

For a single line, the flow rate is:

$$I_{hi} \cdot \dot{Q}_i = P_{1i} - P_{2i} - r_{hi} \cdot Q_i \tag{14}$$

The pressure change in the second piston is given by:

$$\dot{P}_{2i} = \frac{B}{V_{2i}} \cdot (Q_i - \dot{x}_{2i} \cdot S_{2i}) \tag{15}$$

This leads to the piston movement:

$$m_{p2i} \cdot \ddot{x}_{2i} = P_{2i} \cdot S_{2i} - F_{diski}(x_{2i}) - c_{2i} \cdot \dot{x}_{2i} \tag{16}$$

It must be stressed that the pressure level P_{2i} can be modulated with the pressure-controlled ABS servo-valves.

This piston movement generates a non-linear force on the disk:

$$F_{disk}(x_2) = f(k_{brake2i}(x_2), x_2) \tag{17}$$

where the non-linear spring characteristics are:

$$\begin{cases} f \equiv 0 & \text{if} \quad x_{2i} < x_i^0 \\ f(x_2) = k_{brake2i}(x_{2i}) \cdot (x_{2i} - x_i^0) & \text{if} \quad x_{2i} \geq x_i^0 \end{cases} \tag{18}$$

Finally, the braking torque on a wheel can be approximated by:

$$\Gamma_{bi} = 2 \cdot R_e \cdot \mu_e \cdot F_{diski} \tag{19}$$

3. SEPARATE CONTROLS DESIGN

3.1. Suspension Control

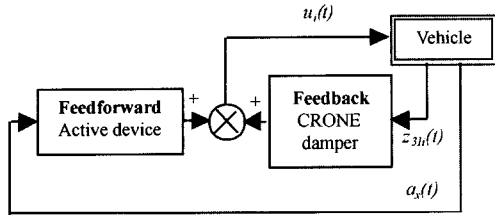It has been shown that the active flow suspension control

Figure 4. Suspension control scheme.

can be designed with feedforward (FF) and feedback (FB) controllers (Moreau *et al.*, 2001) as shown in Figure 4.

With a load leveling active device and a CRONE controlled damper, the expression of the force $u_i(t)$ is the sum of two actions (Moreau *et al.*, 2001). The first one is a feedback action due to the gas spring and the CRONE damper which is, with the help of Laplace transform.

$$U_i^{FB}(s) = C_{si}(s) \cdot Z_{31i}(s) \qquad (20)$$

where the equivalent controller is designed with CRONE methodology:

$$C_s(s) = C_0 \left(\frac{1 + \dfrac{s}{\omega_b}}{1 + \dfrac{s}{\omega_h}} \right)^{n_{susp} - 2} \qquad (21)$$

The second action is a feedforward force developed by the self-leveler system and given by:

$$\frac{U_i^{FB}(s)}{Q_{si}(s)} = \frac{C_{si}(s)}{S_{vi}s} \qquad (22)$$

according to Figure 5 block diagram.

3.1.1. Feedback control

The CRONE feedback (FB) control (Oustaloup and Matthieu, 1999) uses a fractional derivative order n_{susp} of the flow as described in equation (21). This design drastically reduce the system sensitiveness to vehicle mass variations (Moreau, 1995). The fractional derivative order n_{susp} is the single parameter to optimize (Moreau, 1995), through which the compactness of the CRONE control is illustrated. Thus a linear quadratic criteria is introduced:

$$J = \lim_{T \to \infty} \frac{1}{T} E \left\{ \int_0^T \left(\begin{array}{c} \alpha_1 r_1(t)^2 + \alpha_2 r_2(t)^2 + \\ + \alpha_3 r_3(t)^2 \end{array} \right) \cdot dt \right\} = \sum_{i=1}^{3} \alpha_i \cdot J_i \qquad (23)$$

where

$$\begin{cases} r_{1i}(t) = z_{3i} - z_{1i}(t) \\ r_{2i}(t) = z_{1i}(t) - z_{0i}(t) \\ r_3(t) = \ddot{z}_{3i} z_{1i}(t) \end{cases} \qquad (24)$$

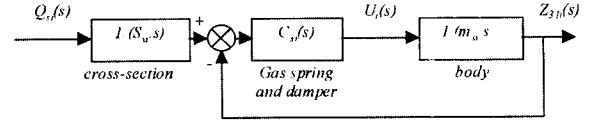Figure 5. Suspension force block diagram.

With Parseval's equality, (21) becomes (Moreau, 1995):

$$J_i = \lim_{T \to \infty} \frac{1}{T} E (\int_0^T r_i(t)^2 dt) = h v_x \int_{-\infty}^{+\infty} |H_i(j\omega)|^2 d\omega \qquad (25)$$

The associated transfer functions.

$$\{H_i(s)\} = \left\{ \frac{Z_{31}(s)}{V_0(s)}; \frac{Z_{10}(s)}{V_0(s)}; \frac{A_2(s)}{V_0(s)} \right\} \qquad (26)$$

give the images of suspension deflection for suspension function, tire deflection for road holding, and body vertical acceleration for passengers comfort.

The optimal control problem can thus be formulated as finding:

$$m^{opt} = n_{susp}^{opt} - 2 = \arg \min_m J \qquad (27)$$

Two strategies are then derived (cf. Fig. 6). The first one is a comfort oriented strategy:

$$(\alpha_1 = 1; \ \alpha_2 = 1; \ \alpha_3 = 20) \qquad (28)$$

$$\lfloor m_1^{opt} = 0, 564; \ m_2^{opt} = 0, 586 \rfloor \ comfort \qquad (29)$$

and the second one is a road holding oriented strategy:

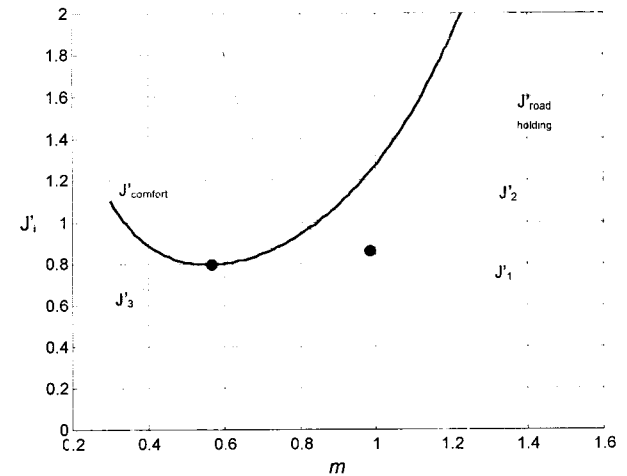$$(\alpha_1 = 1; \ \alpha_2 = 20; \ \alpha_3 = 1) \qquad (30)$$

Figure 6. Optimal suspension normalized criteria for —— comfort oriented strategy and ------ road holding oriented strategy.
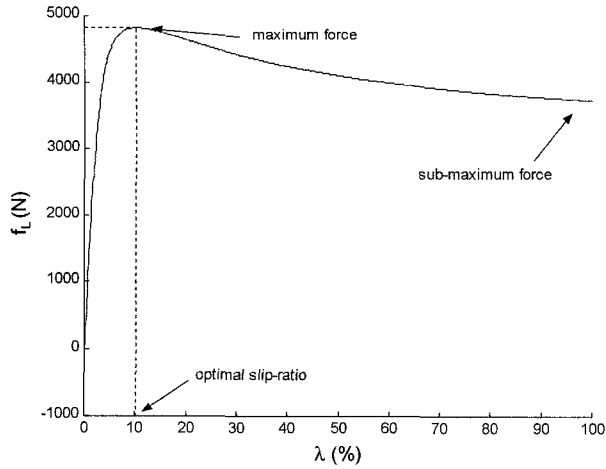
Figure 7. Braking force vs. slip-ratio on a dry road.

$$\lfloor m_1^{opt}=0,982; \quad m_2^{opt}=0,938 \rfloor \quad road\ holding \qquad (31)$$

3.1.2. Feedforward control

For maximum comfort, the pitch has to be minimized. This can be achieved by rejecting the load shifts with the active device such that:

$$u_i^{FF}(t)=-f_{0i}(t) . \qquad (32)$$

Assuming an acceleration sensor is available, the load shifts f_{0i} can be derived by inverting equation (5). Then with equation (22), the suspension flows for active disturbance rejection can be calculated.

3.2. ABS Control

Purpose of ABS. To understand the basis of tire physics, the braking force dependency to the slip-ratio is illustrated in Fig. 7, for a standard load and a coefficient of friction of 1.When the wheel is locked, the braking force is always less than the maximal force where the maximal force is obtained for a single slip-ratio value said to be the optimal value. Thus, ABS control consists of regulating the slip-ratio near the optimal value to maximize the braking force by modulating the brake pressures.

3.2.1. ABS simplified model

To design a controller, a simplified model has to be derived according to (Jacquet, 1996; Assadian, 2001). A model composed of a quarter car, in Figure 8, will be used for controller design.

The wheel dynamic is given in equation (7); and the longitudinal dynamic is obtained from equation (6) as follows:

$$m \cdot \dot{v}_x=f_{Li}(\mu,\lambda_i,F_{zi}) \qquad (33)$$

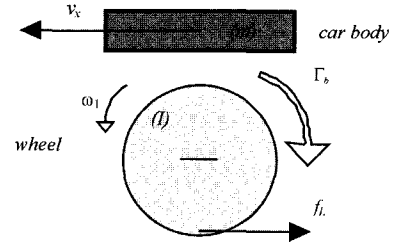In a linear steady-state behavior, with equations (15-19),

Figure 8. ABS simplified model.

the relation between the torque and the pressure becomes:

$$\Gamma_{bi}=K_{ei} \cdot P_{2i} \qquad (34)$$

with the static gain due to previous simplifications:

$$K_{ei}=\frac{2 \cdot R_e \cdot \mu_e \cdot k_{2i}^0 \cdot S_{2i}}{k_{2i}^0 + \dfrac{B \cdot S_{2i}}{V_{2i}}} \qquad (35)$$

To simplify again, the brake pressure is the sum of two sources, namely:

$$P_{2i}=P_{1i}-P_{ABSi} \qquad (36)$$

The pressure-controlled servo-valves are assumed to have a bandwidth about 100 Hz large enough to be modeled as a constant gain factor, namely:

$$P_{ABSi}=H_{brake0} \cdot \Gamma_{ABSi} \qquad (37)$$

The ABS uses the wheel speeds provided by sensors at each wheel, as illustrated in the control block diagram of Figure 9. The control problem can be described as a wheel speed regulation given a slip-ratio reference.

3.2.2. Feedforward control

As previously stated, the ABS purpose is to regulate the slip-ratio (Ref block in Figure 9). This can be achieved by inverting (8):

$$\omega_{ref}=\frac{\hat{v}_x}{R}(1 - \lambda_{ref}) \qquad (38)$$

assuming vehicle speed is measured or estimated.

In many approaches, the optimal slip-ratio is kept constant about 10%. However, Pacejka's model shows
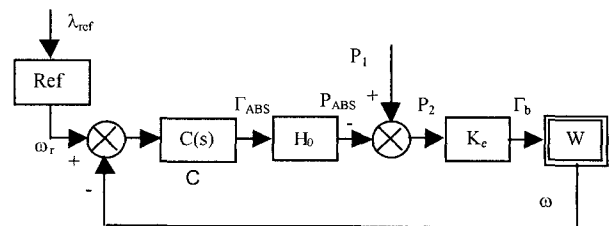

Figure 9. ABS control scheme.

that the slip-ratio reference is also highly dependent on the road coefficient of friction. The key idea of the feedforward (FF) control is that when the ABS has switched on, the vehicle deceleration is near (but non-equal to) optimal deceleration. Then, assuming an acceleration sensor is available, the ABS can have an image of the road coefficient of friction and then adapt the slip-ratio reference to achieve optimal deceleration (Assadian, 2001).

Hence, using equations (6) and (9) with the same friction coefficient for rear and front axles, one can write for near maximal deceleration:

$$a_x = \mu \cdot g \tag{39}$$

Thus with experimental data, a parabolic interpolation between the values of optimal slip-ratios and vehicle acceleration is constructed:

$$\lambda_{opt} = \gamma_2 a_x^2 + \gamma_1 a_x + \gamma_0, \tag{40}$$

where parameters γ_j only depend on tire characteristics.

3.2.3. Feedback control

The major difficulty for designing the feedback (FB) controller is the non-linearity associated with the tire response (W block in Figire 9). Equation (7) can be written as:

$$\frac{\dot{\omega}_{1i}(t)}{\Gamma_{bi}(t)} = \frac{1 - \delta_i(t)}{I_i} \tag{41}$$

with the introduction of a new variable:

$$\delta_i(t) = \frac{R_i \cdot f_{Li}(t)}{\Gamma_{bi}(t)} \tag{42}$$

This variable represents the tire non-linear response dependent on the tire-road coefficient of friction, which is an uncertain parameter. However, as we deal with a physical dissipative system, δ_i can be bounded. With the help of simulations, it can be inferred that:

$$0 \leq \delta_i \leq 0.97 \tag{43}$$

Introducing the equivalent inertia I_{eqi} (Jacquet, 1996) :

$$I_{eqi} = \frac{I_i}{1 - \delta_i} \tag{44}$$

the Laplace transformation of equation (41) provides:

$$\frac{\omega_{1i}(s)}{\Gamma_{bi}(s)} = \frac{1}{I_{eqi} \cdot s} \tag{45}$$

The non-linear non-stationary plant has then been transformed into a linear stationary plant of equation (43) with an uncertain bounded parameter. Then, the ABS control has to be robust to the variations of the equivalent inertia to guarantee stability of the actual plant (Tsypkin et al., 1994).

According to Figure 9 and equation (43), the plant is defined as:

$$G(s) = \frac{H_{brake0} \cdot K_e}{I_{eq} \cdot s} \tag{46}$$

A second-generation CRONE controller can be designed to enforce the following form for the open-loop transfer function (Jacquet, 1996):

$$\beta(j\omega) = C_0 \cdot \left(\frac{1 + \frac{j\omega}{\omega_b}}{\frac{j\omega}{\omega_b}}\right)^2 \cdot \left(\frac{1 + \frac{j\omega}{\omega_h}}{1 + \frac{j\omega}{\omega_b}}\right)^{n_{ABS}} \cdot \frac{1}{1 + \frac{j\omega}{\omega_h}} \tag{47}$$

This form includes a fractional derivative behavior of order n_{ABS} around the crossover frequency enabling a phase margin constancy therefore a robust performance (Oustaloup and Matthieu, 1999).

3.2.4. ABS logic

It must also be paid attention to ABS activations. ABS must be activated before a wheel locks and must be desactivated when the driver releases the brake pedal. To this end, events are defined. When the slip-ratio exceeds the optimal slip-ratio λ_{opt} over a constant given value $\Delta\lambda$, the wheel is going to lock and the ABS is activated. A second event is defined for desactivating the ABS: the
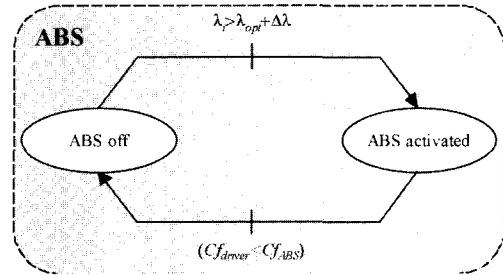

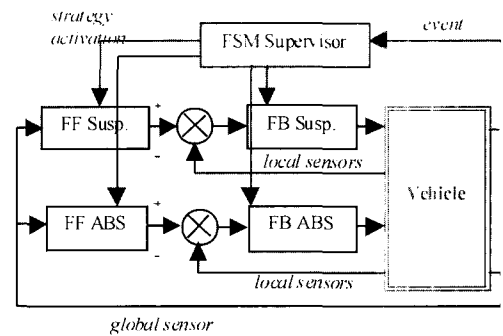Figure 10. ABS finite state machine logic.

Figure 11. Hybrid architecture for a cooperative control between ABS and suspension systems.
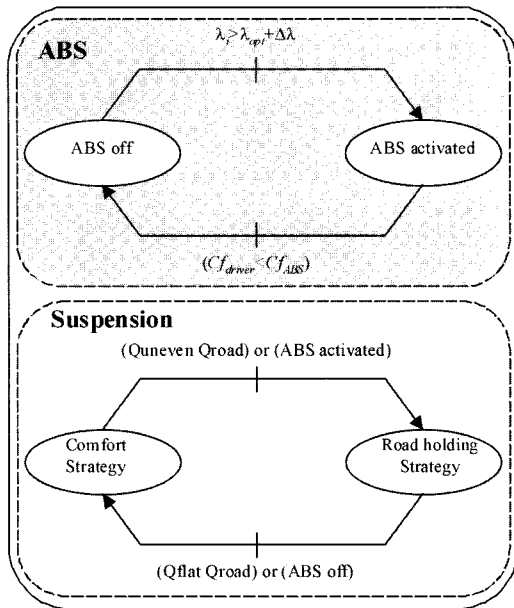
Figure 12. FSM supervisor for a cooperative control between ABS and suspension systems.
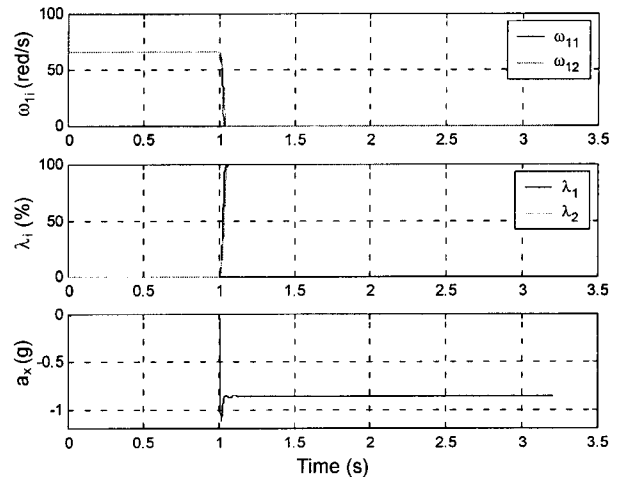

Figure 13. Wheel rotational speeds, slip ratios and vehicle deceleration when braking without ABS on an even road.

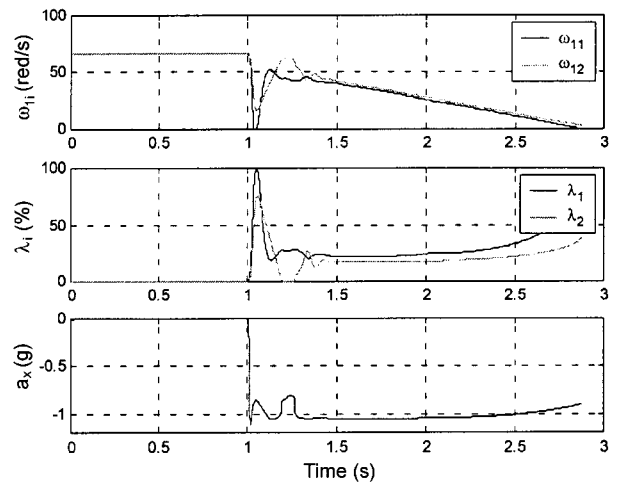Figure 14. Wheel rotational speeds, slip ratios and vehicle deceleration when braking with ABS on an even road.

driver brake torque demand is compared to the torque caused by the ABS system. The associated finite state machine is given in Figure 10.

4. COOPERATIVE CONTROL DESIGN

4.1. Cooperative Strategy

ABS aims to minimize the stopping distance when switched on. Thus, the suspension control can also be switched in a road holding oriented strategy to maximize the tire normal forces helping to generate maximum braking forces according to (9). This idea leads to the hierarchical hybrid control (Riedinger, 1999) between the two subsystems in Figure 11. This architecture must be considered as a proposition for a global vehicle control (Abadie, 1999), based on a FSM supervisor (Koutsoukos and Antsaklis, 1999).

The suspension strategy must be changed according to the road state of surface. In case of a smooth road, the road holding strategy is then preferred. However, when the ABS is activated, the situation is said to be critical. Comfort is no longer a priority, the suspension must be switched on the road holding strategy. These considerations lead to the design of the FSM supervisor described in Figure 12.

4.2. Performance

To understand the performance of such a hybrid control, three series of tests are simulated. The first set deals with braking on a flat road with and without ABS. The second

one compares suspension strategies when braking with ABS on an uneven road. The last one sums up the hybrid control comparing the braking distances.

4.2.1. ABS tests on an even road

The car (a *Citroën Xantia*) is driven on a dry and flat road. The driver hits the pedal (full braking) after one second. This causes the wheels to lock without ABS intervention (cf. Figure 13). Nevertheless, when ABS is activated, the slip-ratios are controlled avoiding wheel locking, which enables to rise vehicle deceleration (cf. Figure 14) and then to reduce the stopping distances by 10% in this case.
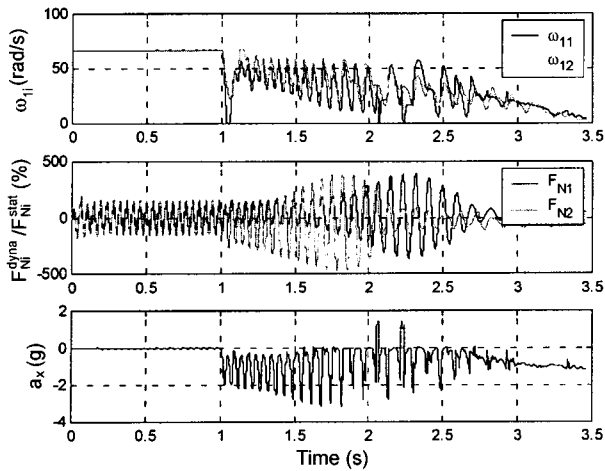
Figure 15. Wheel rotational speeds, relative tire normal forces and vehicle deceleration when braking with ABS on an uneven road with comfort oriented suspension strategy.
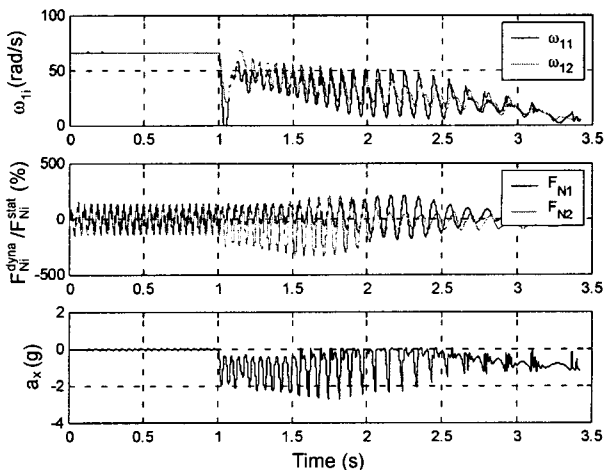

Figure 16. Wheel rotational speeds, relative tire normal forces and vehicle deceleration when braking with ABS on an uneven road with road holding oriented suspension strategy.

4.2.2. Suspension strategy comparison

The same situation is simulated with a dry and uneven road (the ABS is activated). As the comfort oriented suspension strategy favors vehicle body movement filtering, the tire normal forces are degraded compared to the road holding strategy (cf. Figure 15 and Figure 16). As a consequence, the road holding strategy enable to reduce the vehicle deceleration variations due to the unevenness of the road helping to reduce the stopping distance by 2, 5% in this particular case.
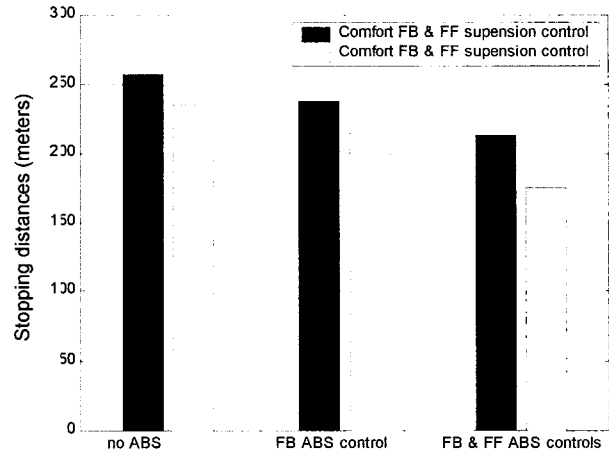

Figure 17. Stopping distances for the different controls of the hybrid architecture.

4.2.3. Overall performance for the cooperative strategy

The performances of the several controls are then compared with simulation results at full braking on a icy and uneven road in Figure 17. These results show that a cooperative control (road holding suspension strategy with ABS) can drastically reduce the stopping distance.

5. CONCLUSIONS

The separate and cooperative controls for ABS and suspension have shown the benefits of a three steps design: feedforward, feedback controllers and FSM logic. This leads to a hybrid hierarchical architecture that enhances vehicle global performance. This architecture appears to be generic and will be extended in the future work.

REFERENCES

Abadie, V. (1998). Continuously-variable damping system. Patent No. 98400985.2, PSA Peugeot Citroën.

Abadie, V. (1999). Architectures de commande de systèmes pilotés dun véhicule automobile. Journées Automatique & Automobile. Octobre 1999. LAP ENSEIRB Université Bordeaux I, France.

Assadian, F. (2001). Mixed H ∞ . and fuzzy logic controllers for the automobile ABS. PSA Peugeot Citroën. SAE Technical Paper Series 2001-01-0594. SAE 2001 World Congress, March 5-8, 2001, Detroit, Michigan, USA.

Dreyer, A., Gräber, J., Hoffman, M., Rieth, P. et Schmitt, S. (1992). Structure and function of the brake and suspension control system, BSCS. SAE Paper No. 925078, pp. 7–17.

Forkenbrock, G., Flick, M. and Garrott, R. W. (1998). A comprehensive light vehicle antilock brake system test track performance evaluation. *SAE Paper No. 1999-01-1287.*

Hamrs, K. (2001). Perspectives in automotive control. Robert Bosch GmbH. *3rd IFAC Workshop,* Advances in Automotive Control, March 28–30, 2001, Karlsruhe, Germany.

Jacquet, C. (1996). Modélisation et Commande CRONE d'un système de freinage avec antiblocage (ABS) pour véhicule automobile. DEA *LAP Université Bordeaux I* ENSEIRB, France.

Koutsoukos, X. D. and Antsaklis, P. J. (1999). Design of hybrid system regulators. *Proceedings of the 38th Conference on Decision & Control,* Phoenix, Arizona, USA.

Moreau, X. (1995). La dérivation non entière en isolation vibratoire et son application dans le domaine de l'automobile. La suspension CRONE : du concept à la réalisation. LAP, Université Bordeaux I.

Moreau, X., Nouillant, C. and Oustaloup, A. (2001). Effect of the CRONE suspension system on braking.

LAP Université Bordeaux I, PSA Peugeot Citroën. *3rd IFAC Workshop,* Advances in Automotive Control, March 28-30, 2001, Karlsruhe, Germany, 63–68.

Oustaloup, A. et Matthieu, B. (1999). La commande CRONE, du scalaire au multivariable. *Edition Hermès,* Paris. ISBN 2-7462-0043-0.

Pacejka, H. B. and R. S Sharp. (1991). Shear force development by pneumatic tires in steady-state conditions : A review of modeling aspects. *Vehicle Systems Dynamics,* **20,** 121–176.

Riedinger, P. (1999). Contribution à la commande optimale des systèmes dynamiques hybrides. Thèse de doctorat, *CRAN -Institut National Polytechnique de Lorraine,* France.

Tsypkin, Y. Z., Hill, D. J. and Isaksson, A. J. (1994). A Frequency-domain robust instability criterion for time-varying and non-linear systems. *Automatica,* **30,** **11,** 1779–1783.

Wright, P.G. and D.A. Williams. (1989). The case for an irreversible active suspension system. *SAE Paper No. 890081,* 83–90.